Available online at www.sciencedirect.com

ScienceDirect

Proceedings of the Combustion Institute 37 (2019) 4371–4378

Proceedings of the Combustion Institute

www.elsevier.com/locate/proci

Mechanism and kinetics of Cu_2O oxidation in chemical looping with oxygen uncoupling

Mingze Su [a], Jie Cao [a], Xin Tian [a], Yongliang Zhang [b], Haibo Zhao [a,*]

[a] State Key Laboratory of Coal Combustion, Huazhong University of Science and Technology, Wuhan 430074, PR China
[b] State Key Laboratory of Power Systems, Department of Thermal Engineering, Tsinghua University, Beijing 100084, PR China

Received 30 November 2017; accepted 21 June 2018
Available online 23 August 2018

Abstract

In chemical looping with oxygen uncoupling, oxygen carrier (OC) circulates between the fuel and air reactors to release and absorb O_2 repeatedly. In order to assess the re-oxidation characteristic of Cu-based OC in the air reactor from the microscopic mechanism and macroscopic kinetics perspective, DFT calculations and isothermal oxidation experiments were conducted. In DFT calculations, $Cu_2O(111)$ surface was chosen as the objective surface to explore the oxygen uptake as well as the atomic transportation pathways, and to determine the rate-limiting steps basing on the energy barrier analyses. It was found that the energy barrier of the surface reaction step (0.96 eV) is smaller than that of the ions diffusion step (1.61 eV). Moreover, the Cu cations outward diffusion occurs more easily than O anions inward diffusion, which confirmed the epitaxial growth characteristic of Cu_2O oxidation. The isothermal oxidation experiments were conducted in a thermogravimetric analyzer (TGA), and about 3.5 mg $CuO@TiO_2$-Al_2O_3 particles within the diameter range of 75–110 μm were tested between 540 and 600 °C, where the internal and external gas diffusion effects were eliminated. Mixtures of 5.2-21.0 vol.% O_2 in N_2 were adopted as the gas agent for oxidation. Based on the understandings obtained from DFT calculations, a simple mathematical model with unknown parameters of the surface reaction process (mainly the activation energy, E_k) and ions diffusion process (mainly the activation energy, E_D) was established to describe the overall oxidation process in TGA experiments. Eventually, these unknown parameters were determined as $E_k = 50.5$ kJ/mol and $E_k = 79.2$ kJ/mol via global optimization. With the attained parameters, simulations reproduced the experimental results very well, which demonstrated that this simplification model, where grain is converted almost layer by layer but different from the feature of the shrinking core model is able to accurately describe the overall oxidation process of Cu_2O.

Keywords: Chemical looping with oxygen uncoupling; Cu_2O oxidation; Mechanism and kinetics; DFT calculation

1. Introduction

Chemical looping combustion (CLC) [1,2], which has the characteristic of CO_2 inherent separation, has been raised to be a promising Carbon

* Corresponding author.
E-mail address: hzhao@mail.hust.edu.cn (H. Zhao).

https://doi.org/10.1016/j.proci.2018.06.162

Capture and Storage (CCS) technology. In CLC, air is replaced by oxygen carrier (OC) to oxidize fuels. Some metal oxides, such as CuO, Mn_2O_3, and Co_3O_4, which are able to release gaseous O_2 at high temperatures and oxygen-deficient conditions, can be used as OC materials for chemical looping with oxygen uncoupling (CLOU) [3]. As a special kind of CLC process, CLOU mainly uses gaseous O_2 released by the OC to oxidize fuels. Among all the tested OC materials for CLOU, Cu-based OCs exhibit high oxygen transport rate and oxygen donating capacity within typical CLOU temperature window (800-1000 °C), and therefore have been recognized as an excellent OC candidate for CLOU. In CLOU, CuO decomposes to Cu_2O first and then regenerates itself via the re-oxidation reaction ($Cu_2O + 1/2O_2 \rightarrow 2CuO$).

There have been many publications focusing on either macrocosmic thermo-chemical performance in batch-operated [4] and interconnected fluidized bed reactors [5] or microcosmic kinetics [6–8] and mechanism [9,10] of the reduction process of Cu-based OC. Whereas, this work focused on the regeneration of OC in CLOU, i.e., the oxidation process of Cu_2O, which is also of great importance to the whole chemical looping system.

Up to now, the oxidation characteristics of Cu_2O to CuO at medium and high temperature have been experimentally investigated. It was found that the product layer (CuO) is epitaxial growth at the surface and dominated by the outward diffusion of cations, where the driving force is dependent on the oxygen potential gradient across the oxide scale [11–13]. Nevertheless, the proposed kinetic models are always discrepant. Zhu et al. [13] investigated the oxidation of Cu_2O to CuO at 600-1050 °C under ambient atmosphere, and their kinetic model follows a logarithmic rate law. While Park and Natesan [14] pointed out that the parabolic rate law should be applied to describe the oxidation of Cu_2O to CuO. Quantitatively, Chuang et al. [15] determined an intrinsic activation energy of 55 kJ/mol for the oxidation of Cu_2O to CuO, by eliminating many influencing factors such as the internal and external gas diffusion. While Adánez-Rubio et al. [8] claimed that the same reaction which was also controlled by chemical kinetics had an activation energy of 32 kJ/mol. These discrepancies may be originated from different experimental factors, and a consensus dynamic description of the oxidation process is thus hard to be established. In this sense, it is urgent to clarify these ambiguous understanding of the Cu_2O oxidation process with more underlying and common knowledge.

The reactivity of Cu_2O oxidation is intrinsically dependent on the electron and crystal structures. Hence, an atomic modeling within the quantum chemistry method may effectively demonstrate the detailed reaction pathway information and energy profile of every constituent elementary steps in the Cu_2O oxidation process, which is very important for the development of reaction kinetic model. However, DFT calculation has limitations in its computational cost aspect (cannot deal with large atomic system) and fundamental theory aspect (only the ground-state structures can be treated and cannot consider the effect of oxygen partial pressure). Consequently, it is almost impossible to establish a macroscopically applicable reaction kinetic model directly. Conventionally, the direct fitting to the experimental results combining with the macroscopic level gas-solid reaction model, e.g., apparent model, shrinking core model, etc., can gives kinetic parameters like the activation energy, pre-exponential factor, reaction order and some specific parameters in the gas-solid reaction models. One of the disadvantages of the conventional approach is that many influencing factors cannot be distinguished clearly, which will hardly contribute to a clear understanding on Cu_2O oxidation mechanism and kinetics. Constructing the mathematical model with unknown parameters to describe the reaction process and then conducting a global optimization calculation to fit these unknown parameters has been proven to be a good approach for reaction kinetic analysis [6,16,17]. In this approach, how to construct a reasonable mathematical model and how to define the interval of the unknown parameters are the two key issues. Fortunately, DFT calculation can help to solve the aforementioned two issues.

In this study, we tried to investigate the oxidation mechanisms of Cu_2O to CuO by DFT calculations, aiming to reveal the oxygen uptake as well as the atomic transportation pathways. Moreover, the rate-limiting steps were also determined, basing on the energy barriers analyses. Isothermal oxidation experiments were then conducted in a thermogravimetric analyzer (TGA). Meanwhile, based on the analysis of the internal and external diffusion effect and the understandings attained from DFT calculations, a simple mathematical model was established to describe the overall conversion process of the samples in TGA. Through global optimization, parameters of the surface reaction and atomic diffusion were determined. Some conclusions from DFT calculation were also confirmed by the experimental analysis. These fundamental insights are beneficial to the comprehensive understanding of the intrinsic re-oxidation characteristics of Cu-based OC in the air reactor, and can also provide theoretical support to the multi-scale research in CLOU. This study "bridges" the microscopic mechanism and macroscopic kinetics, being ready for exploring oxidation/reduction mechanism and kinetics of other oxygen carriers.

2. Methods

2.1. DFT calculation

All DFT calculations were conducted using the CASTEP (Cambridge Serial Total Energy Package) [18] program package. The generalized gradient approximation (GGA) in the form of Perdew-Wang (PW91) was chosen for the electron exchange-correlation energy. The interactions of electron and ion were modeled by the ultra-soft pseudo-potential, and the Brillouin zone interactions were described within the Monkhorst-Pack type mesh of $4 \times 4 \times 1$. Before formal calculations, some convergence tests of the energy cutoff and k-points separation were conducted (see Section S1 in Supplemental Material (SM)), accordingly, 400 eV and 0.04 were selected for the above two parameters in the formal calculations. The well-known GGA + U method was adopted to describe the strong electron correlations of transition-metals. 7.5 eV was chosen for U (corresponding to the Cu 3d orbital), which was also suggested by previous study [19].

With the above introduced method and settings, the Cu_2O unit cells were optimized first and the geometry structure is shown in Fig. S5a, SM. $Cu_2O(111)$ surface was chosen as the objective surface in this study, for which is the most stable low-index Cu_2O surface containing compact Cu-O layers under ambient conditions [20]. Three-layers $Cu_2O(111)$ (2×1) slab model was built through cleaving its bulk phase. The vacuum gap was set to be 20 Å, and the bottom layer was fixed in calculations. Periodic boundary condition was adopted for all boundaries. The optimized slab is shown in Fig. S5b, SM. Before oxygen adsorption calculation, the O_2 molecule structure was optimized in a 20 Å × 20 Å × 20 Å cubic vacuum box to minimize the periodicity effect.

In this study, the adsorption energy of O_2 molecule on the surface, E_{ad}, was defined as:

$$E_{ad} = E(O_2/slab) - [E(O_2) + E(slab)] \quad (1)$$

here, $E(O_2)$ and $E(slab)$ are the total energies of the free O_2 molecule and bare slab, respectively; $E(O_2/slab)$ presents the total energy of the adsorption structure. When searching for the reaction pathway, the complete LST/QST approach (linear/quadratic synchronous transit) was used to find out the transition state (TS) as well as to calculate the energy barrier, E_b, which was defined as:

$$E_b = E(TS) - E(IS) \quad (2)$$

where, $E(TS)$ and $E(IS)$ are the energies of the transition state and the initial state, respectively.

2.2. Experimental approach

Experiments were conducted in a thermogravimetric analyzer (SETARAM-S60). The hierarchically-structured $CuO@TiO_2$-Al_2O_3 OC proposed by our research group was used as the testing sample. The detailed preparation method of the OC was briefly described in Section S2 of SM and can also refer to [21,22]. This kind of OC allows us to use the active material as few as possible, meanwhile the OC is still in granular state. In this sense, the influence of internal diffusion can be minimized. Before the formal experiment, over 20 redox cycles were conducted to ensure the pore structure of the OC had fully developed. High purity N_2 was used as the gas agent in the oxygen releasing stage, while four kinds of gas agents, 21.0 vol.%, 14.0 vol.%, 10.5 vol.% and 5.2 vol.% O_2 balanced by high purity N_2, were adopted in the re-oxidation stage. In order to minimize the diffusion effect caused by the crucible, 3.5 mg OC particles within the diameter range of 75–110 μm were evenly dispersed on silica wool in each test, and the top surface of which was paralleled with the rim of the crucible. In the oxygen releasing stage, the reaction temperature was 850 °C, while in the re-oxidation stage, the reaction temperatures were 540 °C, 560 °C, 580 °C or 600 °C. The gas flow rate of 180 mL/min was chosen because the oxidation rate of Cu_2O do not change any more at this point with the increase of gas flow rate in preliminary experiments.

3. Results and analysis

3.1. DFT calculations and mechanism analysis

3.1.1. Surface reaction of $Cu_2O(111)$

Firstly, the surface reaction of $Cu_2O(111)$ was studied. The DFT calculation started with putting a free O_2 molecule upon the $Cu_2O(111)$ surface (5 Å distance), and optimizing the composite structure. It was found that the molecule keeps a free status without O–O bond breaking, and this configuration was set as the initial state (IS, $Cu_2O+O_2(g)$) of the reaction. In order to find the potential adsorption sites, the free oxygen molecule was moved toward the surface straightly. All possible sites were tested (see Section S3 in SM), and the most stable site (i.e. with the biggest adsorption energy, $Cu_2O+O_2(ad)$) was determined at last. The calculated adsorption energy is 2.09 eV, which belongs to the strong chemisorption. The following key step of surface oxidation is the dissociation of O_2 molecule. In order to determine the most favorable dissociation pathway, the O–O bond was broken first, and these two O atoms were moved along the horizontal direction to make their distance longer than 3 Å. After optimization, the dissociation configuration with the lowest overall energy was chosen to be the final state (FS, Cu_2O+2O^{2-}) of surface oxidation (see Section S3 in SM). Finally, a TS search calculation was performed to identify

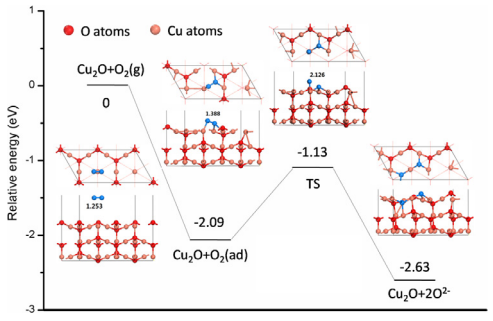

Fig. 1. O_2 molecule adsorption and dissociation process on Cu_2O(1 1 1) slab and the corresponding potential energy diagram. (blue ball: adsorbed O atoms). (For interpretation of the references to color in this figure legend, the reader is referred to the web version of this article.)

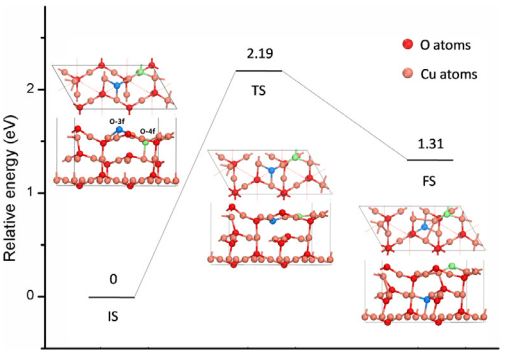

Fig. 2. The structures for O inward diffusion and the corresponding potential energy diagram. (blue ball: O-3f, green ball: O-4f). (For interpretation of the references to color in this figure legend, the reader is referred to the web version of this article.)

the transition state and the corresponding energy barrier.

The potential energy diagram of the whole process is given in Fig. 1. To conclude from both the structure and energy analyses, the Cu_2O(111) surface oxidation process can be summarized as: at the beginning, free O_2 molecule adsorbs on the clean surface and 201.65 kJ/mol (2.09 eV) energy is released. O atoms bond with the adjacent Cu atoms, the length of O–O bond changes from 1.253 Å to 1.388 Å. Then, two O atoms are motivated to migrate and embed into a stable position of Cu_2O(111) surface, the energy barrier is 0.96 eV. In the TS, the O–O bond is broken and the distance between the two O atoms is stretched to 2.126 Å. It should be noted that in the final structure, one separated O anion is threefold-coordinated (O-3f) while another is fourfold-coordinated (O-4f), which is similar to the atoms configuration of CuO(111) surface [7]. The transformation from Cu_2O crystal configuration to CuO crystal configuration indicates that the above surface oxidation pathway in our calculation is reasonable. The whole process is exothermic with a negative reaction energy (−2.63 eV), and it can proceed rapidly for a relatively low energy barrier (0.96 eV).

3.1.2. Ions diffusion in oxidized Cu_2O region

After the surface reaction between O_2 and substrate, an oxidized region with high oxygen potential and relatively low copper concentration is formed. Here, two diffusion processes were considered for subsequent reaction evolution, one is the inward diffusion of the O anion and the other is the outward diffusion of the Cu cation. For the calculations in this part, the final state (Cu_2O+2O^{2-}) of the previous step was treated as the initial state. As shown in Fig. 2, there are two kinds of dissolved O anion, i.e., O-3f and O-4f. In this configuration, it can be found that the larger migration space and fewer constraints of O-3f make it diffuse more easily than O-4f. Thus, the O-3f was chosen as the studied anion and it was moved from the surface to the second layer. The optimized structure via a vertically downward migration pathway, which has the lowest overall energy, was set as the final state (FS) of the O-3f inward diffusion process. In FS, O-3f bonds with the nearest four Cu cations tightly, thus creating a rhombic Cu-O structure as in the IS. At the same time, a reconstructed exterior surface partially recovers to the morphology of Cu_2O(111) surface. In TS, the O-3f migrates from the initial site to a middle place between the surface and subsurface. A positive value of reaction energy (1.31 eV) indicates the endothermic characteristic of the process, and the calculated energy barrier is up to 2.19 eV (as shown in Fig. 2), which means the growth of CuO crystal phase needs to overcome a big resistance.

Similarly, the calculation of Cu cation outward diffusion was also conducted. Two kinds of Cu cation were considered, i.e., Cu-2f and Cu-3f. After comparison, the outward diffusion of Cu-2f was chosen as the more possible process. Fig. 3 shows the details of this process. In FS, some new Cu-O and Cu-Cu bonds are generated, making the surface crowded. In DFT calculation, the reaction energy of Cu diffusion is 0.88 eV and the corresponding energy barrier is 1.61 eV as plotted in Fig. 3, both of which are lower than those in O inward diffusion. The calculation results indicate that Cu cation outward diffusion is energetically more favorable than O inward diffusion. Therefore, the ions diffusion process is more likely to be dominated by Cu cation outward diffusion. The conclusion is also in accordance with the experience that ions with lower ionic radius can diffuse more easily, as the ionic radius of Cu is smaller than that of O, and the lower-coordinated ions (Cu or O) has a smaller ionic radius.

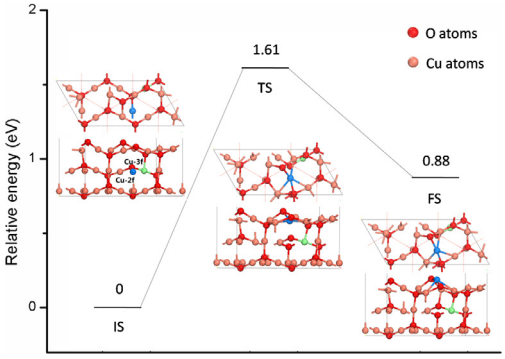

Fig. 3. The structures for Cu outward diffusion and the corresponding potential energy diagram. (blue ball: Cu-2f, green ball: Cu-3f). (For interpretation of the references to color in this figure legend, the reader is referred to the web version of this article.)

As the "Cu diffusion source", Cu cation diffusion in the unreacted bulk region was also calculated (see Section S4 in SM). The results show that this step is not the rate-limiting step.

3.1.3. Cu_2O oxidation mechanism

Based on these DFT calculations, the microscopic mechanism of Cu_2O oxidation may be expressed briefly as: (1) at the initial stage (Fig. 4(P1)), reaction between the clean substrate and O_2 takes place at the gas-solid interface rapidly. A product layer of CuO is produced at the external surface. (2) In the next process (Fig. 4(P2)), as Cu cations outward diffusion is dominant, Cu^+ in sublayer migrates to the exterior surface to balance the copper concentration gradient, meanwhile Cu cations in deep layer migrate upward to fill up the copper vacancies in the sublayer (Fig. 4(P3)). (3) At the same time, the slightly excessive copper cations within the external $Cu_{1+x}O$ layer continue to be consumed by O_2 molecules quickly, which results in the formation of a new product layer at the exterior (Fig. 4(P4)). With the progress of diffusion, the Cu/O ratio of "interior layer" approaches to 1:1 via $Cu_2O + V_{Cu} \rightarrow CuO$, which leads to CuO formation in the bulk phase of the grain.

3.2. Experimental results and kinetics analysis

3.2.1. Experimental results

The measured conversion versus time of Cu_2O oxidation is shown in Fig. 5. There is a relative high conversion rate at the initial stage for all experimental runs, yet the conversion rate decreases afterwards. This is a common phenomenon for heterogeneous non-catalytic reactions. Note that, the conversion rate increases as the temperature and O_2 volume fraction increase.

In these experiments, the elimination of the internal and external diffusion effects has been confirmed by theoretical analysis (more details in Section S5, SM). Thus, in the following work we focus on the evolution of a small grain to investigate the intrinsic oxidation characteristic of Cu-based OCs at the scale of crystalline grain.

3.2.2. Cu_2O oxidation kinetics analysis

From above DFT calculations, it was concluded that Cu cation moves outward to the exterior surface while the O anion remains stationary when Cu_2O is oxidized by O_2. However, the effect of subsequent reconstitution of Cu_2O to CuO when Cu cation leaves away from its original position should also be considered. As the molar volumes of Cu_2O and CuO are different, the reconstitution effect will trigger the volume shrinkage, leading to the convective motion of ions (as schematically shown in Fig. S6, SM). Accordingly, the ions concentration along with radius can be described by the following equations:

$$\frac{\partial C_{Cu}}{\partial t} = -\frac{1}{r^2}\frac{\partial}{\partial r}\left[r^2\left(vC_{Cu} - D_{Cu}\frac{\partial C_{Cu}}{\partial r}\right)\right] \quad (3)$$

$$\frac{\partial C_O}{\partial t} = -\frac{1}{r^2}\frac{\partial}{\partial r}\left[r^2 vC_O\right] \quad (4)$$

where, C_{Cu} and C_O are the molar concentrations of Cu and O ion, respectively; D_{Cu} is the diffusivity of Cu cation; v is the velocity of the convective motion caused by the reconstitution effect. It should be noted that the above equation is used to illustrate the Cu diffusion-induced convective motion of the bulk phase and is only applicable for the inner layers. A reaction source term is required when describing the external surface layer, which will naturally include the effect of the oxygen concentration on the reaction rate.

The molar volume of Cu_2O and CuO is $2.399 \times 10^{-5} (= 2 \times 1.149 \times 10^{-5} + 0.101 \times 10^{-5})$ m^3/mol and $1.250 \times 10^{-5} (= 1.149 \times 10^{-5} + 0.101 \times 10^{-5})$ m^3/mol, respectively. Therefore, the equivalent molar volumes of Cu and O ions for analyzing this mixed system are 1.149×10^{-5} m^3/mol and 0.101×10^{-5} m^3/mol, respectively. In order to close Eqs. (3) and (4), v can be expressed as

$$1.149\left(vC_{Cu} - D_{Cu}\frac{\partial C_{Cu}}{\partial r}\right) = -0.101 vC_O \quad (5)$$

This equation means that the volume fluxes of Cu and O ions are equal at any positions. Unfortunately, although the equations are closed, they are still difficult to be solved. The main reason is that the reaction will result in the grain expansion, and the Eulerian grid is not suitable for this situation. Even if the expansion can be addressed delicately, it is still hard to ensure its accuracy. When substituting Eq. (5) to Eq. (3) or Eq. (4), the equation becomes $\partial C_{Cu}/\partial t = -0.0879 \cdot \partial C_O/\partial t$. It can be seen that in the same control volume, the change rate of Cu cation is far less than that of O anion. Apparently, the result equates to the O anion

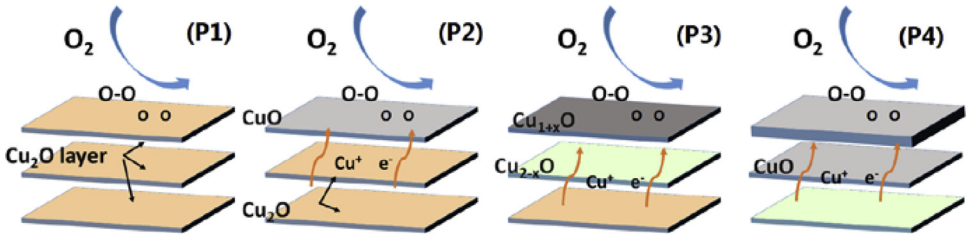

Fig. 4. Schematic view of Cu_2O oxidation mechanism.

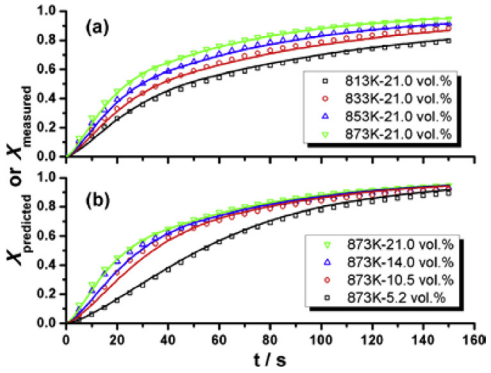

Fig. 5. Measured (symbol) and calculated (line) conversion profile for Cu_2O exposed to (a) different temperatures and (b) different atmospheres.

inward "diffusion", although the O inward movement is not a real diffusion process microscopically. Hence, the following simplifications were made to solve this problem: neglecting the molar concentration change of Cu cation in the control volume and allowing O anion to diffuse from the reaction surface to the bulk phase of the grain. As the concentration of O anion increases, the local oxidation conversion increases. Therefore, a phenomenological diffusivity of O anion was introduced as $vC_O = -D_O \partial C_O/\partial r$. Taking account of C_{Cu} is constant, Eq. (4) was finally converted into the following form:

$$\frac{\partial X}{\partial t} = \frac{1}{r^2}\frac{\partial}{\partial r}\left(r^2 D_O \frac{\partial X}{\partial r}\right) + \Omega r \le r_{grain} \tag{6}$$

where, X represents the Cu_2O conversion; $\Omega = kN_s\theta[O_2]S/(C_{Cu}\Delta V|_{r=r_{grain}})$ is the source term only for the external grid introduced by the surface reaction; $\theta = 1 - X|_{r=r_{grain}}$ is the area fraction of Cu_2O on the external reaction surface of the grain; k is the reaction rate constant; N_s is the moles of Cu per unit of grain external surface; $[O_2]$ is the molar concentration of O_2; S represents the external surface area of the grain; $\Delta V|_{r=r_{grain}}$ is the volume of the external grid. Note that, some parameters have physical significance but their true values are difficult to be determined. For calculation concern, these parameters were assembled to the rate constant, thus the source term can be expressed as $\Omega = k'\theta[O_2]S/\Delta V|_{r=r_{grain}}$.

Before simulations, X was set to be 0 for all computational cells. Zero gradient condition was adopted for both $r = 0$ and $r = r_{grain} = 300$ nm.

Equation (6) and the above boundary and initial conditions form a complete description to the oxidation process of the Cu_2O, where k' and D_O are the only unknown parameters for each experimental run. When the Arrhenius equation is used to express the two unknown parameters, only four parameters, i.e., A_k, E_k, A_D and E_D are unknown for all experimental runs. The simulated solid conversion can be expressed as $X_{predicted} = \int X \cdot dV / \int dV$.

The partial differential equation in Eq. (6) was discretized in the finite volume method form. The global optimization process was under a Simulated Annealing Algorithm control, and the self-adaptive method proposed by Vanderbilt et al. [23] was used to improve the computational efficiency. The unknown parameters were adjusted to minimize the differences between the simulated and measured conversions over all data points: $f = \sum_{\text{alltests}} \sum_{0<t<t*} \sqrt{(X_{predicted} - X_{measured})^2}$. The fitting process is schematically shown in Fig. S7 of SM.

The ranges of the unknown parameters should be determined before the fitting process. According to the results of above DFT calculation, the ranges were set as $A_k \sim [1.0 \times 10^{-12}, 5.0 \times 10^{-7}]$, $E_k \sim [3.0 \times 10^4, 8.0 \times 10^4]$, $A_D \sim [1.0 \times 10^{-12}, 5.0 \times 10^{-7}]$ and $E_D \sim [6.0 \times 10^4, 2.0 \times 10^5]$.

The fitting process resulted in $A_k = 4.86 \times 10^{-8}$, $E_k = 5.05 \times 10^4$, $A_D = 2.41 \times 10^{-12}$ and $E_D = 7.92 \times 10^4$, and the simulated conversion versus time profiles are also shown in Fig. 5. It can be seen that the simulations predict the experimental results very well.

The simulated conversion versus normalized radius at different time points under the condition of 580 °C, 21.0 vol.% O_2 are shown in Fig. 6. It is obvious that the conversions are nonuniformly distributed: initially, the conversion at the external surface of the grain increases quickly, while the oxidation of Cu_2O in the center of the grain does not occur until 40 s.

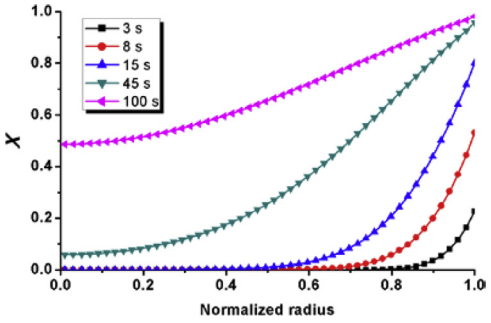

Fig. 6. Simulated conversion vs. normalized radius profiles for Cu_2O exposed to 580 °C, 21.0 vol.% O_2 at selected times.

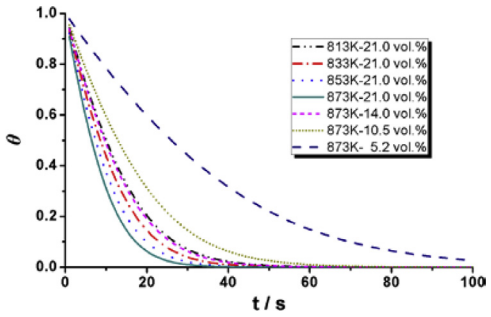

Fig. 7. Surface coverage of Cu_2O at different conditions.

The area fraction of Cu_2O on the external surface of the grain, θ, versus time under different conditions is shown in Fig. 7. It can be seen that θ drops rapidly and is close to 0 before 60 s in most cases. However, for the reaction condition of 580 °C and 5.5 vol.% O_2, θ is still not close to 0 after 100 s. The faster decline of θ demonstrates the shorter time of the surface reaction influencing the overall conversion process. Thus, the influencing time of the surface reaction decreases as the temperature and the O_2 concentration increases.

In Adánez-Rubio's previous work [8], it was found that the effect of the oxygen concentration on the oxidation rate of Cu_2O at low oxygen concentration was higher than that at high oxygen concentration. The proposed model can also predict the different effect of the oxygen concentration. When the sample is exposed in a low oxygen concentration atmosphere, the surface reaction rate is comparable with the ions diffusion rate. As the oxygen concentration increases, the surface reaction rate increases, thus the oxidation degree of the external surface layer of the grain is become higher; Simultaneously, the ions diffusion rate will also increase as the driving force of diffusion is also increased obviously; eventually, the overall reaction rate will increase obviously. However, when the sample is exposed in a high oxygen concentration atmosphere, the surface reaction rate is high enough (the external surface layer of the grain is oxidized almost completely) and the overall reaction rate is controlled by the ions diffusion process. In this condition, as the oxygen concentration increases, the oxidation degree of the external surface layer does not obviously change. Thus the oxygen concentration shows a relatively "smaller" effect on the overall reaction rate.

4. Discussion

The following facts can be confirmed from the above DFT calculations and TGA experiments. (1) In the Cu_2O oxidation process, the surface reaction process is faster than the ions diffusion process. (2) Two stages can be distinguished in the overall oxidation process. At the first stage, the overall process is influenced both by the surface reaction process and the ions diffusion process. Meanwhile, oxidation film is formed rapidly, leading to the influence of the surface reaction reduced. While at the second stage, the overall oxidation process is only dominated by the ions diffusion process.

The activation energy of the ions diffusion is larger than that of the surface reaction, thus the ions diffusion rate could increase faster than the surface reaction rate with the increasing of temperature. As a result, the diffusion resistance may be relatively smaller than the surface reaction resistance at higher temperature condition.

Obvious difference inactivation energies (or the energy barriers) obtained by DFT simulations and experimental kinetics analysis was observed. It could be ascribed to the different scales of the two methods investigated, as well as the limitation of DFT calculation. In the kinetics analysis, a phenomenological O diffusivity was introduced to simplify the fitting procedure, yet there is no corresponding process in DFT calculations. The experimental approach focused on the statistical effects of the migration of enormous ions, while the DFT calculation focused on specific migration pathways of a specified ion. Additionally, in actual processes, ions may also migrate along with the interphase routes once the product phase, CuO, was generated. Limited by the fundamental theory and the computational capability, DFT calculation can not reflect the reality of the physicochemical process in a global sense, which will also introduce inaccuracy to the simulation result. As an example, it is difficult for the DFT calculation in this work to consider the reconstitution effect of Cu_2O to CuO after Cu cation leaves, because a low oxidation degree slab model was adopted. Although a high oxidation degree slab model can be used to investigate the reconstitution effect, yet the information of the initial oxidation stage will miss, additionally, the reconstitution simulation, with huge computational cost, is beyond our computational ability.

In this work, the intrinsic kinetics was obtained in relatively low temperature conditions in which the diffusion effect can be eliminated. We take the view that the intrinsic kinetics proposed can be used to represent the intrinsic oxidation at relevant temperatures for the CLOU process (900–950 °C). Further work should be done to give a comprehensive description to the Cu_2O oxidation process in actual CLOU conditions. Certainly, the internal and external diffusion effect should be considered.

5. Conclusions

The mechanism of the oxidation of Cu-based OC with low-valence state in CLOU was studied via DFT calculation in a microscopic perspective. Meanwhile, isothermal experiments were subsequently conducted in a thermogravimetric analyzer for validating the DFT simulation results and seeking for an applicable reaction kinetic model. The major conclusions are as follows: (1) the oxidation process of the $CuO@TiO_2$-Al_2O_3 OC is controlled by chemical kinetics under the conditions of $T < 600$ °C, $X_{O2} < 21$ vol.%. (2) the oxidation product is epitaxial growth at the surface and the overall process is dominated by the outward diffusion of Cu cation. (3) the surface reaction step is faster than the ions diffusion step, which result in that the oxidation film forms rapidly at the external surface of the grain in the initial stage. With the growth of the oxidation film, the overall process was gradually dominated by ions diffusion step. (4) Cu cation diffusion process together with $Cu_2O \rightarrow CuO$ reconstitution process result in the change rate of Cu cation concentration far less than that of O anion concentration locally. Thus, a model containing phenomenological O anion inward diffusion step and surface reaction step is able to approximate the overall oxidation process, and the activation energies of such two processes are 79.2 kJ/mol and 50.5 kJ/mol, respectively.

Acknowledgements

This work was founded by "National Key R&D Program of China (No. 2016YFB0600801)" and "National Natural Science Foundation of China (No. 51522603)".

Supplementary materials

Supplementary material associated with this article can be found, in the online version, at doi: 10.1016/j.proci.2018.06.162.

References

[1] J. Adanez, A. Abad, F. Garcia-Labiano, P. Gayan, L.F. de Diego, *Prog. Energ. Combust. Sci.* 38 (2012) 215–282.
[2] J. Adanez, A. Abad, T. Mendiara, P. Gayán, L.F. de Diego, F. García-Labiano, *Prog. Energ. Combust. Sci.* 65 (2018) 6–66.
[3] T. Mattisson, A. Lyngfelt, H. Leion, *Int. J. Greenh. Gas Con.* 3 (2009) 11–19.
[4] S.Y. Chuang, J.S. Dennis, A.N. Hayhurst, S.A. Scott, *Combust. Flame* 154 (2008) 109–121.
[5] A. Abad, I. Adánez-Rubio, P. Gayán, F. García-Labiano, L.F.D. Diego, J. Adánez, *Int. J. Greenh. Gas Con.* 6 (2012) 189–200.
[6] E.A. Goldstein, R.E. Mitchell, *P. Combust. Inst.* 33 (2011) 2803–2810.
[7] S.Y. Chuang, J.S. Dennis, A.N. Hayhurst, S.A. Scott, in: G. Yue, H. Zhang, C. Zhao, Z Luo (Eds.), 20th International Conference on Fluidized Bed Combustion, Springer, Berlin, Heidelberg, 2009, pp. p512–p518.
[8] I. Adánez-Rubio, P. Gayán, A. Abad, F. García-Labiano, L.F. de Diego, J. Adánez, *Chem. Eng. J.* 256 (2014) 69–84.
[9] Y. Zhang, H. Zhao, L. Guo, C. Zheng, *Combust. Flame* 162 (2015) 1265–1274.
[10] H. Zhao, Y. Zhang, Y. Wei, J. Gui, *P. Combust. Inst.* 36 (2017) 4069–4077.
[11] Z. Grzesik, M. Migdalska, *High Temp. Mat. Pr-ISR* 30 (2012) 277–287.
[12] A. Li, H. Song, J. Zhou, X. Chen, S. Liu, *Crystengcomm* 15 (2013) 8559.
[13] Y. Zhu, K. Mimura, M. Isshiki, *Oxid.Met.* 62 (2004) 207–222.
[14] J.H. Park, K. Natesan, *Oxid. Met.* 39 (1993) 411–435.
[15] S.Y. Chuang, J.S. Dennis, A.N. Hayhurst, S.A. Scott, *Energ. Fuel.* 24 (2010) 3917–3927.
[16] Z. Zhao, M. Uddi, N. Tsvetkov, B. Yildiz, A.F. Ghoniem, *J. Phys. Chem. C* 120 (2016) 16271–16289.
[17] H. Randall, A. Ralf Doepper, A. Renken, *Ind. Eng. Chem. Res.* 36 (1997) 2996–3001.
[18] J.P. Perdew, J.A. Chevary, S.H. Vosko, et al., *Phys. Rev. B* 46 (1992) 6671–6687.
[19] J. Hu, D. Li, J.G. Lu, R. Wu, *J. Phys. Chem. C* 114 (2010) 17120–17126.
[20] Z. Gao, W. Huang, L. Yin, L. Hao, K. Xie, *Catal. Lett.* 127 (2009) 354–359.
[21] Z. Xu, H. Zhao, Y. Wei, C. Zheng, *Combust. Flame* 162 (2015) 3030–3045.
[22] X. Tian, Y. Wei, H. Zhao, *Fuel* 209 (2017) 402–410.
[23] D. Vanderbilt, S.G. Louie, *J. Comput. Phys.* 56 (1984) 259–271.